A Series of Redox Active, Tetrathiafulvalene-Based Amidopyridines and Bipyridines Ligands: Syntheses, Crystal Structures, a Radical Cation Salt and Group 10 Transition-Metal Complexes

Thomas Devic, Narcis Avarvari,* and Patrick Batail*[a]

Abstract: Amidopyridine and −2,2′-bipyridine derivatives of EDT-TTF and BTM-TTF (EDT = ethylenedithio, BTM = bis(thiomethyl), TTF = tetrathiafulvalene) have been synthesized and crystallographically characterized. In the solid state, the different supramolecular organization of all these donors results from the competition between the intermolecular interactions, that is, van der Waals, hydrogen-bonding, π–π stacking, and donor–acceptor interactions. The electron-donating properties of the new donors have been investigated by cyclic voltammetry measurements. A radical cation salt, formulated [EDT-TTF-CONH-*m*-Py]$^{\bullet+}$[PF_6]$^-$, has been prepared by electrocrystallization and its crystal structure determined by X-ray analysis. Square planar dicationic complexes with the same donor and $M^{II}L_2$ fragments (M = Pd, Pt, L_2 = bis(diphenylphosphino)propane (dppp) or bis(diphenylphosphino)ethane (dppe)) have been synthesized and one of them, containing the Pd(dppp) unit, has been structurally characterized. The conformation of the complex in the crystalline state is *anti*, with the coexistence of the *dl* racemic pair of enantiomers.

Keywords: amides · electrocrystallization · hydrogen bonds · palladium · tetrathiafulvalenes

Introduction

The synthesis and coordination chemistry of electro-active molecules functionalized by various mono- or polydentate ligands have developed steadily during the past decade. For example, pyridine,[1] bipyridine,[2] and terpyridine[3] derivatives of ferrocene have been synthesized and engaged in transition-metal complexes, whose spectroscopic properties in solution are influenced by the oxidation of ferrocene into ferricinium. Another prominent redox-active class of compounds is represented by tetrathiafulvalene (TTF) derivatives, which have been extensively studied in the search for molecular conductors and superconductors.[4] The association of a TTF core with heteroatom-based ligands, capable of coordinating to a metallic center, offers a whole novel perspective on the modulation of architecture and collective electronic properties of molecular solids. Hence, the metal may serve as a template in order to assemble two or more TTF units, by means of metal–-ligand interactions, in a rigid predefined manner ruled by the coordination geometry and the number of free coordination sites. In addition, the functional redox ligands may be further activated and assembled into electroactive supramolecular edifices by electrocrystallization experiments. Such radical cation salts would provide unique models to probe the structural and electronic consequences of mixing the metal d and ligand π electrons and spins in their frontier orbitals. Hence, depending on the strength of the intramolecular transfer integral between two or more such redox functionalities bound to the metal center with respect to the HOMO–LUMO splitting of the complex, internal redox processes coupled to structural instability may occur in the solid state—an eventuality of much current interest.[5] In addition, when the coordinated metal is paramagnetic, the coexistence of magnetic and conducting properties hold much promise for the development of bifunctional molecular materials, a field of much current activity.[6,7] Various TTF derivatives containing coordinating groups, such as crown ethers,[8] thioethers,[9] phosphines,[10] and stibines,[11] along with the corresponding metal complexes, have been described in the literature so far. Nevertheless, among the TTF ligand systems the most extensively studied by several groups are those containing pyridine or bipyridine ligands. Thus, TTF, methyl-TTF, BEDT-TTF (BEDT = bisethylenedithio) and tetrakis(thioalkyl)-TTF derivatives functionalized with pyridine and bipyridine have been synthesized either by phosphate-mediated coupling reactions of the appropriate 1,3-dithiole-2-ones or 1,3-dithiole-

[a] Dr. T. Devic, Dr. N. Avarvari, Dr. P. Batail
Laboratoire Chimie, Ingénierie Moléculaire et Matériaux d'Angers
UMR 6200 CNRS-Université d'Angers, Bât. K
2 Boulevard Lavoisier, 49045 Angers (France)
Fax: (+33) 241-735-405
E-mail: narcis.avarvari@univ-angers.fr
patrick.batail@univ-angers.fr

Supporting information for this article is available on the WWW under http://www.chemeurj.org/ or from the author.

 DOI: 10.1002/chem.200305776

2-thiones,[12] or by reacting TTFs that contain reactive groups and functionalized pyridines or bipyridines. This last group of reactions includes Stille cross-coupling reactions,[13] Wittig reactions,[14] and utilization of the tetrathiolate [TTF-S_4]$^{4-}$[15] or dithiolate [TTF-S_2]$^{2-}$ ions,[16] generated from protected precursors under basic conditions, by nucleophilic substitutions with halogenalkylpyridines or -bipyridines. Paradoxically, transition-metal complexes involving a TTF-pyridine ligand[17] and the first example of a radical cation salt have been reported only very recently.[18]

Here we report on the utilization of the amide function as a spacer between redox active TTF cores and nitrogen-containing heterocycles (Scheme 1).

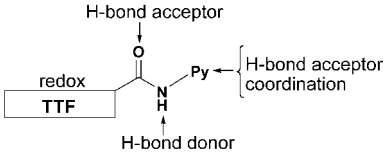

Scheme 1. TTF-amido-pyridines: schematic drawing illustrating the role of each functionality.

Elaborating from the known capacity of amides to form recurrent hydrogen-bond patterns in crystals,[19] situations can be created in which intra- and intermolecular hydrogen-bonded amide–amide linkages compete in the solid state with intermolecular p_π–p_π overlap interactions and van der Waals interactions. In a series of monocomponent solids and radical cation salts based on the mono-[20] and diamides[21] of EDT-TTF (EDT-TTF = ethylenedithiotetrathiafulvalene), this feature has demonstrated the many benefits of engaging such functional precursors for directing the solid-state chemistry and collective electronic properties of molecular solids.[21,22] Of particular note, is the observation in the former series that the hydrogen-bond donor–acceptor character of the amide group appended to a TTF core changes upon oxidation of neutral TTF in the radical cation.[23] Thus, we reasoned that the TTF-amide-pyridine triad should have an interesting potential as synthon for the construction of crystalline molecular materials. Note also that, a very recent study has shown that the host–guest recognition in solution, through hydrogen bond formation, between a TTF-amido-pyridine and different complementary guests can be electrochemically controlled.[24] In the solid state we expect that the hydrogen-bond interactions will compete with S···S van der Waals and π–π overlap interactions, as well as with the coordination properties of these ligands, directed towards the synthesis of new molecular bricks.

Herein we report the synthesis and structural characterization of a series of EDT- and *o*-BTM-TTF-amidopyridines (*o*-BTM = *ortho*-bis(thiomethyl)) and amidobipyridines, one radical cation salt, and Pd^{2+} and Pt^{2+} complexes of one of these donors, the first examples of transition-metal complexes of a TTF-pyridine ligand based on these metallic centers.

Results and Discussion

Synthesis and X-ray structures of EDT-TTF-CONH-pyridines and -2,2′-bipyridine: Our first choice concerning the TTF derivative type to be explored was the EDT-TTF (ethylenedithiotetrathiafulvalene), with respect to the interesting results obtained in the EDT-TTF-amides series.[21,22] Indeed, from a material point of view it is worthwhile to preserve the ethylenedithio bridge on one side of the TTF core, as its ability to establish more lateral S···S and p_π–p_π intermolecular interactions directs the stabilization of solid-state constructs with either one- or two-dimensional electronic structures and a rich low-dimensional physics.[25] Thus, EDT-TTF-COCl (**1**) reacts[20] with *meta*-aminopyridine, *para*-aminopyridine and 5-amino-2,2′-bipyridine,[26] respectively, to yield *meta*- and *para*-amidopyridine, as well as 5-amido-2,2′-bipyridine derivatives of EDT-TTF, as depicted in Scheme 2.

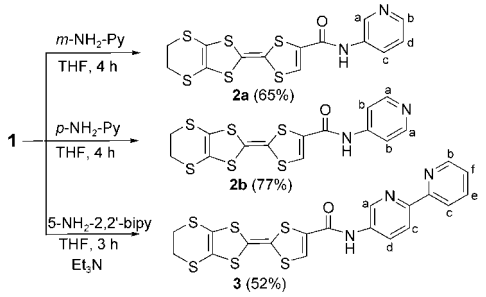

Scheme 2. Synthesis of EDT-TTF-CONH-*m*-Py (**2a**), EDT-TTF-CONH-*p*-Py (**2b**) and EDT-TTF-CONH-5–2,2′-bipy (**3**).

All three compounds were obtained as single crystals and the analysis of their structures determined by X-ray diffraction allowed us to decipher a set of intermolecular interactions detailed in the following. Each donor bears hydrogen-bond acceptors, namely carbonyl and pyridyl groups, as well as one strong (NH) and one weaker (vinyl CH) hydrogen-bond donor. In the neutral, non-coordinated state, one expects[20,21] intermolecular hydrogen bonds to be an important factor in governing the solid-state arrangement, in competition with S···S van der Waals interactions, and, eventually, π–π stacking between aromatic rings. Also, interactions of the donor–acceptor (i.e., TTF–pyridine) type can be expected within the crystalline structures of these compounds. As a means of tracking the balance of the competing interactions in this series of compounds, it is convenient to consider the dihedral angle ϕ between the pyridine and TTF mean planes, as well as the three dihedral angles θ_1, θ_2, and θ_3 about the C–C, C–N, and N–C bonds, respectively, as defined in Scheme 3.

Compound **2a** crystallized in the orthorhombic system, space group *Pbca*, with one donor molecule in general position and one acetonitrile molecule disordered on an inversion center. Selected bond lengths and angles, which are all within the normal range, are given in Table 1.

An ORTEP diagram of the TTF derivative is shown in Figure 1a. The π-donor molecule is planar (ϕ = 5.71(12)°,

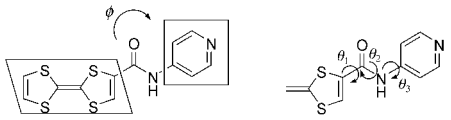

Scheme 3. Intramolecular dihedral angles in the TTF-amido-pyridine system.

Table 1. Selected bond lengths [Å] and angles [°] for **2a**, [**2a**]PF_6 and [Pd(dppp)(**2a**)$_2$](OTf)$_2$.

	2a·0.5 MeCN	(**2a**)PF_6·THF	[Pd(dppp)(**2a**)$_2$]-(OTf)$_2$·$CHCl_3$·Et_2O
C1–C2	1.327(4)	1.343(7)	1.343(11)
C1–C9	1.483(4)	1.483(7)	1.481(11)
C9–O1	1.222(3)	1.213(6)	1.218(9)
N1–C10	1.411(3)	1.411(6)	1.388(10)
S1–C1	1.756(3)	1.744(5)	1.775(8)
S2–C2	1.727(3)	1.714(5)	1.723(9)
C3–C4	1.343(4)	1.407(7)	1.331(10)
C2-C1-C9	130.6(2)	131.8(5)	129.8(8)
O1-C9-N1	123.4(3)	125.6(5)	123.3(8)
O1-C9-C1	118.7(2)	118.0(5)	121.3(8)
N1-C9-C1	117.9(3)	116.4(5)	115.4(8)
C9-N1-C10	126.1(2)	126.3(4)	123.0(8)

$\theta_1 = 1.8(4)°$, $\theta_2 = 4.6(5)°$, $\theta_3 = 11.4(4)°$) and forms ribbons, running along the *b* direction, through intermolecular hydrogen bonds (Figure 1b). Molecules form centrosymmetric dimers between two ribbons.

A neat, outer hydrogen-bond backbone provides the ribbon cohesion out of the nitrogen atom (N2) of a pyridine moiety and the N1–H1 and C2–H2 groups of a neighboring molecule, wrapped up into a $R_2^1(7)$[27] cyclic pattern (Table 2). This pincer, already observed in the structure of other TTF-amides,[20] albeit in those cases the acceptor was the carbonyl oxygen atom, is reinforced by an additional weaker hydrogen bond with the C11–H11 group. Note the dual activation of atom H11, a consequence of its location in *para* to atom N_2 and *ortho* to the amido group. Note also that the carbonyl oxygen atom O1 is involved only in an intramolecular interaction with C14–H14.

Compound **2b** crystallized in the monoclinic system, space group $P2_1/c$, with one planar molecule ($\phi = 5.13(7)°$, $\theta_1 = 1.1(5)°$, $\theta_2 = 0.8(7)°$, $\theta_3 = 6.3(7)°$) in a general position. This donor organizes in one-dimensional infinite chains by means of hydrogen bonds; however, in striking contrast to the *meta* isomer **2a**, the carbonyl oxygen atom now plays the role of the acceptor, whereas the pyridine nitrogen atom is engaged in no noticeable hydrogen bond and the vinylic CH acts as donor instead of the amidic hydrogen (Figure 2a). This behavior may be a consequence of the lower basicity of the pyridine nitrogen atom, due to its location in *para* to the electron withdrawing amido group. Nevertheless, in the crystalline structure of a related compound, namely *p*-Ph-CONH-Py, strong hydrogen bonds of NH···N(Py) type have been observed.[28] Therefore the lack of such interactions in **2b** is likely to result from the present net packing efficiency of these planar motifs, since the occurrence of a NH···N bond would require orthogonal cyclic motifs, that is, a significant decrease of the structure compactness.

Interestingly, along the *b* direction molecules stack in a "head-to-tail" manner (Figure 2b), with the pyridine ring sandwiched between two TTF moieties, thus forming a infinite stable -D-A-D-A- assembly (D = donor, A = acceptor), with an average distance between the mean pyridine and TTF planes amounting to about 3.7 Å. Evidently, in this case, the packing of the molecules is driven mainly by these donor–acceptor electrostatic interactions, rather than by the hydrogen bonds emphasized above. Hence, within this class of compounds there is a competition in the solid state between the two types of interactions, and the system will try to accommodate both. Compound **3** crystallized in the monoclinic system, space group $P2_1/n$, with one molecule in a general position. The bipyridine unit has a pronounced twist with respect to the TTF unit ($\phi = 38.91(9)°$), and within it a dihedral angle of 27.73(18)° between the pyridine rings, lying in a *cis* conformation, is observed. The bifurcated hydrogen-bond formed between the amido N1–H1 group of one molecule and the bipyridine N2 and N3 nitrogen atoms of a neighboring molecule is responsible for this, whereas the twist between the pyridine rings is attributed to a second

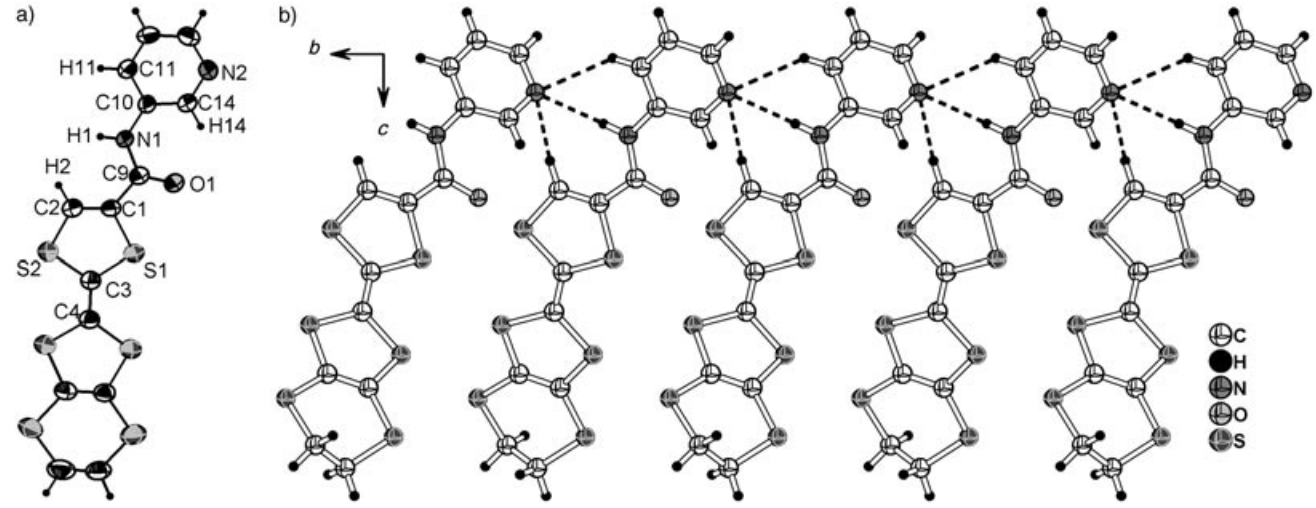

Figure 1. a) ORTEP view of **2a**·0.5 MeCN, with 50% probability displacement ellipsoids; b) one-dimensional hydrogen-bond network in the crystalline structure of **2a**·0.5 MeCN.

Table 2. Hydrogen-bond parameters.

	D−H···A	D···A [Å]	H···A [Å]	D−H···A [°]
2a·0.5 MeCN	$N-H_{amide}\cdots N_{py}$	3.083(3)	2.285	154.4
	$C-H_{vinyl}\cdots N_{py}$	3.328(4)	2.458	155.8
	$C-H_{py}\cdots N_{py}$	3.489(4)	2.727	139.8
	$C-H_{ethylenic}\cdots O_{amide}$	3.227(4)	2.786	108.4
	$C-H_{py}\cdots O_{amide}$ [a]	2.792(3)	2.174	123.0
2b	$C-H_{vinyl}\cdots O_{amide}$	3.543(5)	2.667	157.2
	$C-H_{py}\cdots O_{amide}$ [a]	2.881(5)	2.295	120.6
	$C-H_{ethylenic}\cdots N_{py}$	3.480(4)	2.586	153.3
3	$N-H_{amide}\cdots N_{bipy(1)}$	2.904(4)	2.119	151.3
	$N-H_{amide}\cdots N_{bipy(2)}$	3.526(5)	2.811	141.8
	$C-H_{vinyl}\cdots N_{bipy(2)}$	3.629(5)	2.743	159.1
	$C-H_{bipy(1)}\cdots O_{amide}$	3.265(4)	2.492	140.4
	$C-H_{bipy(1)}\cdots O_{amide}$ [a]	2.884(5)	2.311	119.6
5·CH_2Cl_2	$N-H_{amide}\cdots N_{py}$	3.048(4)	2.209	164.8
	$C-H_{vinyl}\cdots N_{py}$	3.284(5)	2.460	147.5
	$C-H_{py}\cdots N_{py}$	3.499(6)	2.757	137.5
	$C-H_{py}\cdots O_{amide}$	3.271(5)	2.659	123.8
	$C-H_{py}\cdots O_{amide}$ [a]	2.850(6)	2.236	123.0
6·MeOH	$N-H_{amide}\cdots O_{solv}$	2.960(2)	2.018	166.8
	$C-H_{vinyl}\cdots O_{solv}$	3.164(3)	2.245	167.5
	$C-H_{bipy(1)}\cdots O_{solv}$	3.353(3)	2.587	139.4
	$O-H_{solv}\cdots N_{bipy(2)}$	2.753(2)	1.965	165.3
	$C-H_{bipy(2)}\cdots O_{amide}$	3.296(3)	2.614	130.7
	$C-H_{bipy(1)}\cdots O_{amide}$ [a]	2.928(2)	2.392	116.6
	$C-H_{bipy(2)}\cdots N_{bipy(1)}$ [a]	2.784(3)	2.463	100.3
	$C-H_{bipy(1)}\cdots N_{bipy(2)}$ [a]	2.893(3)	2.597	99.0
7·2 Py	$N-H_{amide}\cdots N_{solv}$	3.054(5)	2.212	166.1
	$C-H_{vinyl}\cdots N_{solv}$	3.364(6)	2.459	164.7
	$C-H_{bipy}\cdots N_{solv}$	3.387(6)	2.602	142.5
	$C-H_{solv}\cdots O_{amide}$	3.413(6)	2.505	165.7
	$C-H_{bipy}\cdots O_{amide}$ [a]	2.857(6)	2.291	118.9
	$C-H_{bipy}\cdots N_{bipy}$ [a]	2.811(6)	2.506	99.3
[**2a**]PF_6·0.5 MeCN	$N-H_{amide}\cdots O_{solv}$	2.825(6)	2.034	152.6
	$C-H_{vinyl}\cdots O_{solv}$	3.128(7)	2.334	143.1
	$C-H_{py}\cdots O_{solv}$	3.499(8)	2.870	125.9
	$C-H_{py}\cdots O_{amide}$ [a]	2.834(6)	2.189	125.7
$[Pd(dppp)(\mathbf{2a})_2](OTf)_2\cdot CHCl_3\cdot Et_2O$	$N-H_{amide}\cdots O_{anion}$	2.942(10)	2.188	146.4
		2.960(8)	2.114	167.7
	$C-H_{vinyl}\cdots O_{anion}$	3.039(10)	2.353	130.4
		3.199(9)	2.296	163.6
	$C-H_{py}\cdots O_{amide}$ [a]	2.908(11)	2.550	103.2
		2.852(10)	2.410	109.0
	$C-H_{phenyl}\cdots O_{anion}$	3.077(9)	2.295	141.3
		3.136(10)	2.352	141.9
	$C-H_{py}\cdots O_{anion}$	3.196(10)	2.303	160.7
		3.287(9)	2.441	151.4
	$C-H_{chloroform}\cdots O_{anion}$	3.168(10)	2.214	164.5

[a] Intramolecular interaction.

hydrogen-bond between N3 and C2−H2 group (Figure 3a). Distances and angles for all these interactions are given in Table 2.

The hydrogen-bond pattern discussed above develops along *b* leading to infinite chains, as illustrated in Figure 3b. Note also that the $O_1\cdots H_{11}$ hydrogen bond directs the association of two molecules into dyads along the $a+c$ direction, through a pair of two such hydrogen bonds. Thus, the possibility of this compound to form alternating donor–acceptor stacks in solid state is essentially hampered by the stabilization energy due to the complex set of hydrogen bonds. Indeed, within the stacks along the *b* direction, molecules are staggered one to another, they do not correspond by an inversion center, and, moreover, because of the twist angle ϕ, the donor–acceptor interaction is negligible.

Synthesis and X-ray structures of BTM-TTF-CONH-pyridine and 2,2′-bipyridines: The synthesis of EDT-TTF-CONH-5-2,2′-bipy (**3**) was motivated by the access to a chelating redox active system; yet, it turned out that it was sparingly soluble, which seriously limited further studies in electrocrystallization and coordination. In order to gain higher solubility the ethylene bridge was discarded in favor of two methyl groups to yield the bis(thiomethyl)tetrathiafulvene (BTM-TTF) series. Therefore we synthesized first compound **4**, the bis(thiomethyl) analogue of **1**, by the same method used for the latter (Scheme 4), from the corresponding carboxylic acid **4′**, the X-ray crystal structure of which has been also determined (see Supporting Information for experimental details and crystallographic data).

Then, reaction of **4** with *meta*-aminopyridine and 5-amino-2,2′-bipyridine, by analogy with the reactions described in Scheme 2, affords the corresponding of BTM-TTF-CONH-*m*-Py (**5**) and BTM-TTF-CONH-5-2,2′-bipy (**6**) donors. Both compounds are more soluble than their EDT counterparts. Compound **5** crystallized in the monoclinic system, space group $P2_1/n$, with one donor molecule and one molecule of methylene chloride in general positions. Although **2a** and **5** are not isostructural, their supramolecular organizations through hydrogen bonds are similar and are based on the same type of ribbons, albeit arranged in a slightly different manner. Hence, the crystal structure of **5** will not be detailed any further. In contrast, the hydrogen-bond network and solid-state architecture of **6** differs from that of **3**. Compound **6** crystallized as a solvate, with one molecule of methanol, in the triclinic system, space group $P\bar{1}$. Unlike that of **3**, the geometry of **6** is essentially planar ($\phi = 19.33(8)°$) with no twist between the pyridine rings, arranged in a *trans* manner this time. The methanol of crystallization proves to play a key role in the establishment of the hydrogen-bond network, as its oxygen atom accepts three protons provided by the same donor molecule, whereas the OH proton is involved in a hydrogen bond with one pyridine nitrogen atom from a second

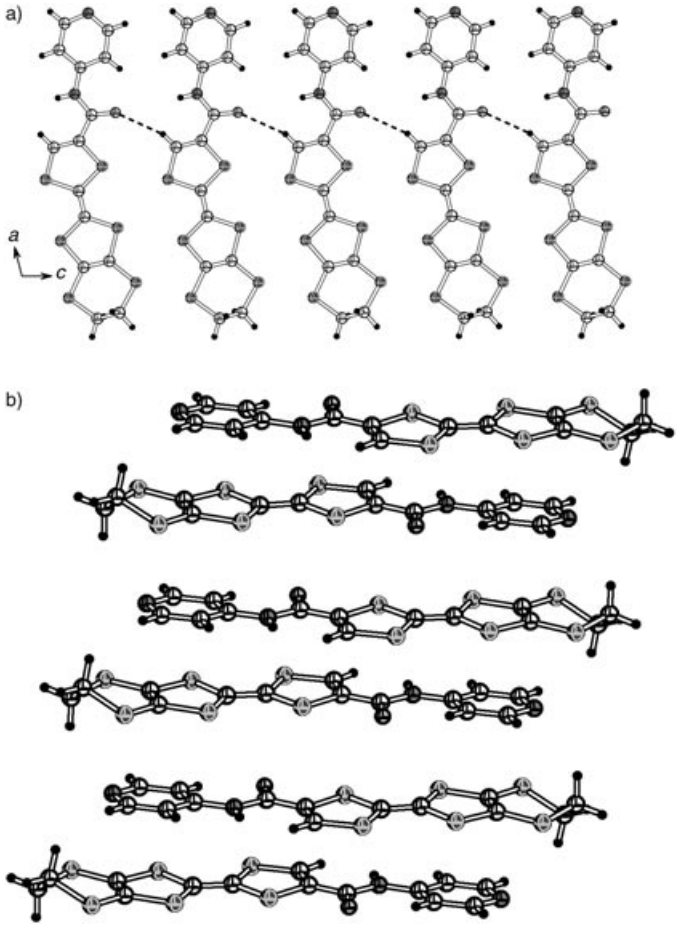

Figure 2. a) Infinite chains mediated by hydrogen bonds in the crystalline structure of **2b**; b) "head-to-tail" stack of molecules **2b**, with a donor–acceptor alternation.

molecule. This pattern leads to the formation of a one-dimensional network running along *a*, as illustrated in Figure 4a. The second pyridine nitrogen atom and the carbonyl oxygen atom are only involved in intramolecular hydrogen bonds (Table 2). The ribbons thus formed organize in an anti-parallel manner along *c* to allow the head-to-tail stacking of the molecules in a staggered arrangement with donor–acceptor (TTF–amidobipyridine) interactions (Figure 4b). The intermolecular mean plane distances within the stacks amount to about 3.7–3.8 Å.

Since the solubility of compound **6** proved to be quite reasonable, the synthesis of a 2,2′-bipyridine bearing two TTF moieties was attempted in order to have a symmetric chelating ligand, a prerequisite to avoid complex stereoisomerism issues in the case of metallic complexes. At the same time, this offers an opportunity to evaluate electronic communication between the two π-donor cores through the bipyridine bridge. Our target compound **7** was synthesized by reacting

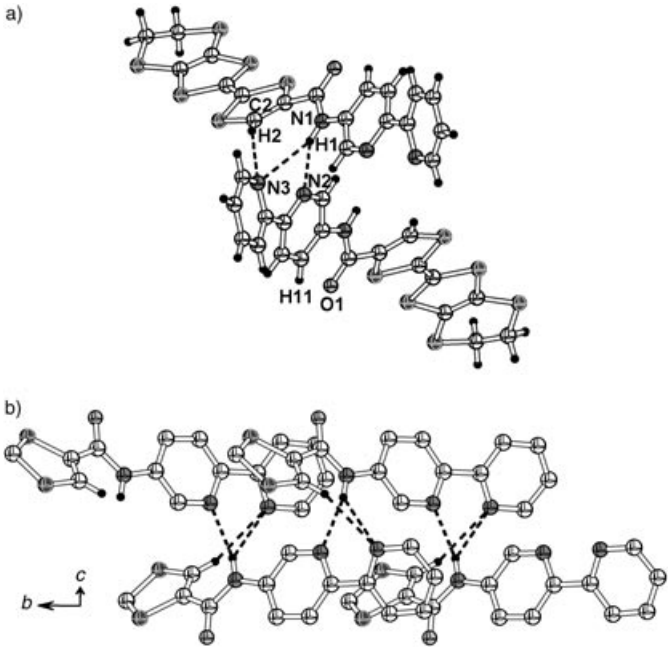

Figure 3. a) NH···N_{Py} hydrogen bonds in the crystalline structure of **3**; b) hydrogen-bond network running along *b* in **3** (only the TTF half bearing the amido-bipyridine group and the protons involved in H-bonding have been represented).

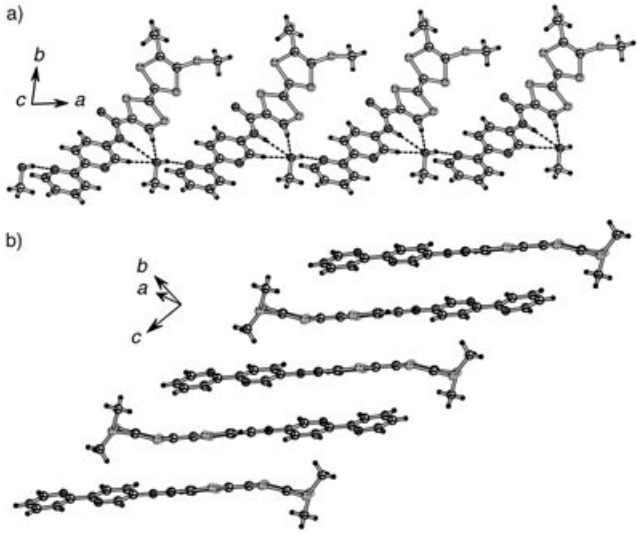

Figure 4. a) Hydrogen-bond ribbon in the crystalline structure of **6**; b) "head-to-tail" stack of donors **6**.

two equivalents of **4** with one equivalent of 5,5′-diamino-2,2′-bipyridine, as described in Scheme 5. The latter compound was prepared starting from 5,5′-dimethyl-2,2′-bipyridine according to a protocol published by the group of Janiak.[29]

Single crystals of **7** were obtained by recrystallization in pyridine and the X-ray structure was determined. The compound crystallized in the monoclinic system, space group

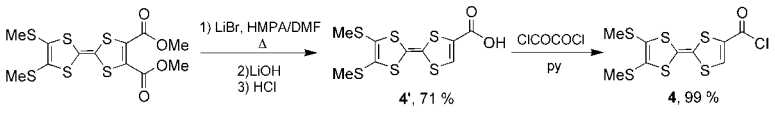

Scheme 4. Synthesis of precursor **4**.

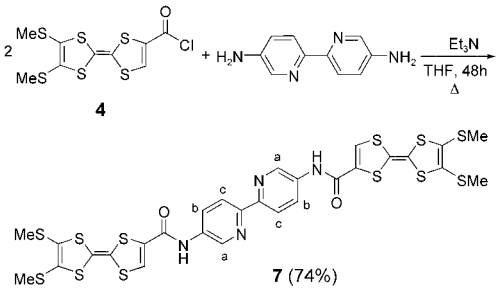

Scheme 5. Synthesis of **7**.

$P2_1/c$, with one half molecule of **7**, which is centrosymmetric, and one pyridine molecule in general positions. The solid-state geometry of the ligand is remarkably planar, with values for dihedral angles as follows: $\phi = 9.61(2)°$, $\theta_1 = 3.4(6)°$, $\theta_2 = 0.7(8)°$, $\theta_3 = 10.8(7)°$, except for the terminal methyl groups *trans* to the molecule mean plane. A three-dimensional hydrogen-bond supramolecular network occurs this time, with the solvent pyridine nitrogen atom acting as acceptor towards vinyl CH, amide NH, and 2,2′-bipy ortho CH; in addition, the carbonyl oxygen interacts with the pyridine solvent *para*-CH, as illustrated in Figure 5a.

Moreover the molecules stack uniformly along *a* in a slightly staggered conformation, with a distance of about 3.6 Å between the mean planes (Figure 5b). Through these different examples discussed so far we have shown that our redox active ligands adapt their crystalline structure to all the rich panel of possible intermolecular interactions, among which the hydrogen bond plays a primordial role.

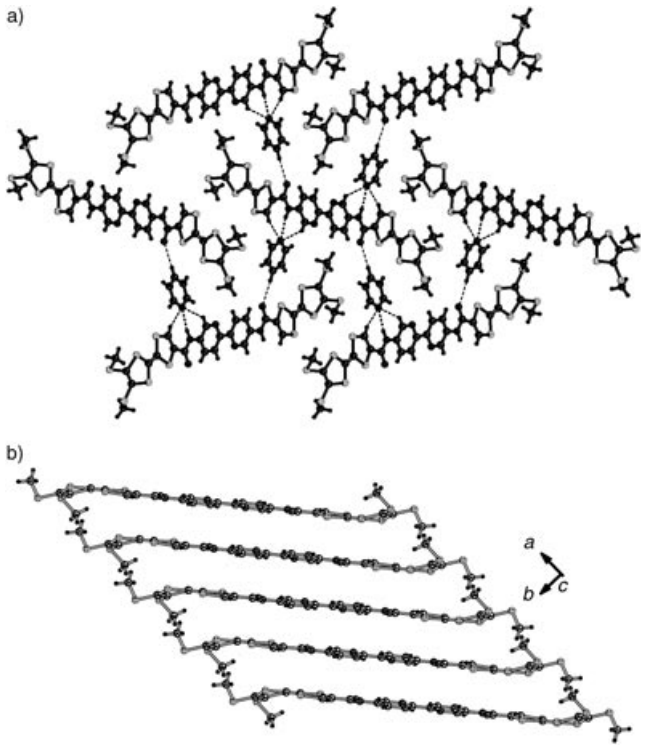

Figure 5. a) Three-dimensional hydrogen-bond network in the crystalline structure of **7**; b) stacking of molecules **7** along *a*.

Redox properties of the donors: In order to evaluate the redox properties of all the donors synthesized so far we have run cyclic voltammetry experiments to determine the oxidation potentials and the reversibility of the processes. The corresponding half-wave potentials for all the compounds along with those of EDT-TTF and EDT-TTF-CONHMe for comparison are listed in Table 3.

Table 3. Oxidation potentials (V vs SCE, nBu$_4$NPF$_6$ 0.05 M in THF at 0.1 V s^{-1}, at 20 °C).

	$E^1_{1/2}$	$E^2_{1/2}$
EDT-TTF[20]	0.59	0.83
EDT-TTF-CONHMe[20]	0.66	0.92
2a	0.66	0.90
2b	0.67	0.92
3	0.66	0.89
5	0.74	0.94
6	0.73	0.93
7[a]	0.75	0.95

[a] Measured in DMF, with a Ag reference electrode.

As expected, both mono-electronic oxidations are fully reversible in the case of mono-TTF donors, with potential values very similar to that of EDT-TTF-CONHMe. Moreover, even in the case of the bis-TTF compound **7**, one can observe also two oxidation reversible waves, each corresponding either to a bi-electronic process or to two successive overlapped mono-electronic processes. Very likely, there is neither an electronic communication between the TTF units through the bipyridine bridge, nor a through space intramolecular interaction, which would have led to a splitting of at least the first oxidation wave.[16b]

Synthesis and crystal structure of [2a]$^{\cdot+}$PF$_6^-$: It has been recently established[23] that, upon oxidation into its radical cation form, the hydrogen-bond donor–acceptor ability of a TTF platform bearing an amide group changes, because its carbonyl group becomes highly deactivated. In the present series of donors there is an additional hydrogen-bond acceptor, namely the pyridine nitrogen atom, and the former analysis of the crystalline structures of the neutral compounds described above has underlined the competition between the two functionalities for directing intermolecular associations. We therefore address the dependence of the hydrogen-bond acceptor character of the pyridine nitrogen atom on the redox state of the molecule, by analysis of the hydrogen-bond network in the crystal structure. Electrocrystallization of **2a** in the presence of the octahedral PF_6^- ion, allowed us to obtain black crystalline plates of a salt formulated as [**2a**]PF_6·THF. The compound crystallized in the triclinic system, space group $P\bar{1}$, with one **2a**$^{\cdot+}$ radical cation, one PF_6^- ion, and a THF molecule in general positions. Selected bond lengths and angles are given in Table 1. As in their neutral form, the organic donors adopt a planar conformation ($\phi = 4.0(2)°$, $\theta_1 = 1.1(7)°$, $\theta_2 = 4.0(9)°$, $\theta_3 = 4.8(9)°$) and organize further into slabs separated by anions and solvent molecules (Figure 6a). The $R_2^1(7)$ hydrogen bond pincer motif, also observed in neutral **2a**, involves amidic

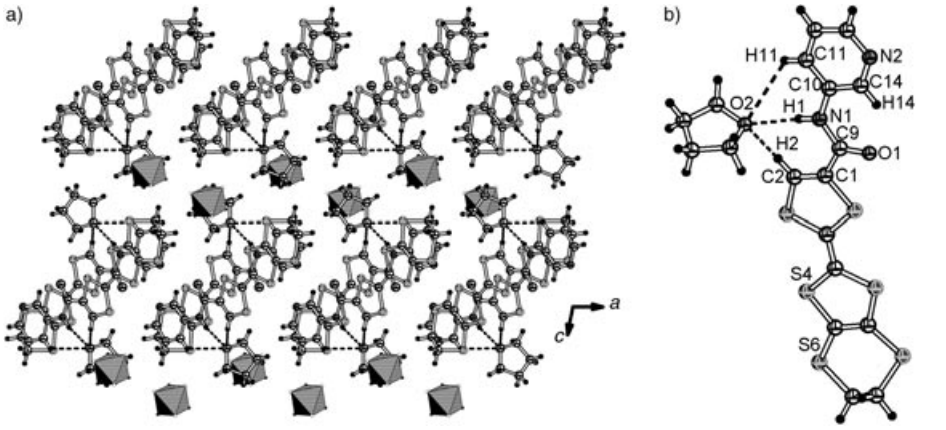

Figure 6. a) Segregated slabs of $\mathbf{2a}^{\cdot+}$ radical cations in the structure of $[\mathbf{2a}]PF_6 \cdot THF$; b) hydrogen bonds THF···$\mathbf{2a}^{\cdot+}$ in $[\mathbf{2a}]PF_6 \cdot THF$.

N–H and vinylic C–H as donors, this time with the THF oxygen atom as acceptor (Figure 6b).

Unlike **2a** and **2b** structures, in this case neither the pyridine nitrogen atom nor the carbonyl oxygen atom engage in hydrogen bonds. This tends to confirm the deactivation of the hydrogen-bond acceptor part in the TTF-based donors upon oxidation in radical cations. As noticed before (vide supra), this phenomenon was already observed and rationalized through electrostatic potential surface theoretical calculations in the case of EDT-TTF-amides salts.[23] Thus, the lack of any active hydrogen-bond acceptor in $\mathbf{2a}^{\cdot+}$ prevents the formation of an extended network, but of isolated ($\mathbf{2a}^{\cdot+}$)-(THF) units (Table 2). Note also the inertness of the anion towards the same type of interaction. As often observed in the case of fully oxidized TTF-based donors, the radical cations strongly dimerize within the slabs, in a "head-to-tail" conformation, to form dicationic $[(\mathbf{2a})_2]^{2+}$ species, as confirmed by the value of the $\beta_{HOMO-HOMO}$ interaction energy overlap calculated by the extended Hückel method (β = 1.2 eV).

Synthesis and characterization of Pd and Pt complexes with 2a: For the coordination chemistry of these new donors, we first focused our attention on the square-planar metallic centers Pd^{2+} and Pt^{2+}, with two *cis* positions occupied by a chelating diphosphine. This kind of precursor, with different linkers between the two phosphino ligands, as for example alkyl chains,[30] ferrocene moiety,[31] crown ethers,[32] or chiral groups[33] have been widely used in the construction of molecular or supramolecular assemblies, by coordinating the remaining free *cis* positions with bipyridine-based ligands.[34] The palladium– or platinum–diphosphine precursors generally used are the bis(triflate) salts, obtained by chlorine abstraction with silver(I) triflate, from the corresponding dichloro derivatives. Thus, $[M(dppp)(OTf)_2]$ (dppp = bis(diphenylphosphino)propane, M = Pd, Pt, OTf = triflate) have been synthesized by the previous procedure[30,35] and further reacted with the donor **2a**. The coordination of the TTF-pyridine at the metallic centers could be easily monitored by ^{31}P NMR spectroscopy. Indeed, in the case of the palladium complex an upfield shift of $\Delta\delta = -16.6$ ppm was observed upon coordination, whereas an even larger downfield shift ($\Delta\delta = 21.0$ ppm) accompanied the reaction with the platinum complex. Interestingly, in the case of the latter, a diasteoisomeric pair (*meso* and *anti-dl* racemic) was formed at room temperature in a ratio 1:1.6, indicating that the rotation barrier is much higher than for the palladium counterpart. This phenomenon was already observed and studied by temperature-dependent ^{31}P and ^{1}H NMR spectroscopy for a large series of mixed bis(phosphine)bis(pyridine)palladium(II) and -platinum(II) complexes.[36] It is likely that the existence of a frozen mixture of diastereoisomers at room temperature in the case of the platinum complex hampered the isolation of single crystals of this compound. In contrast, the palladium complex has a fluxional structure at room temperature on the NMR timescale, and suitable single crystals for X-ray analysis could be grown. The compound crystallized from a mixed chloroform/diethyl ether solvate in the triclinic system, space group $P\bar{1}$, with a molecule of dicationic complex in general position. An ORTEP representation of the molecule is shown in Figure 7a.

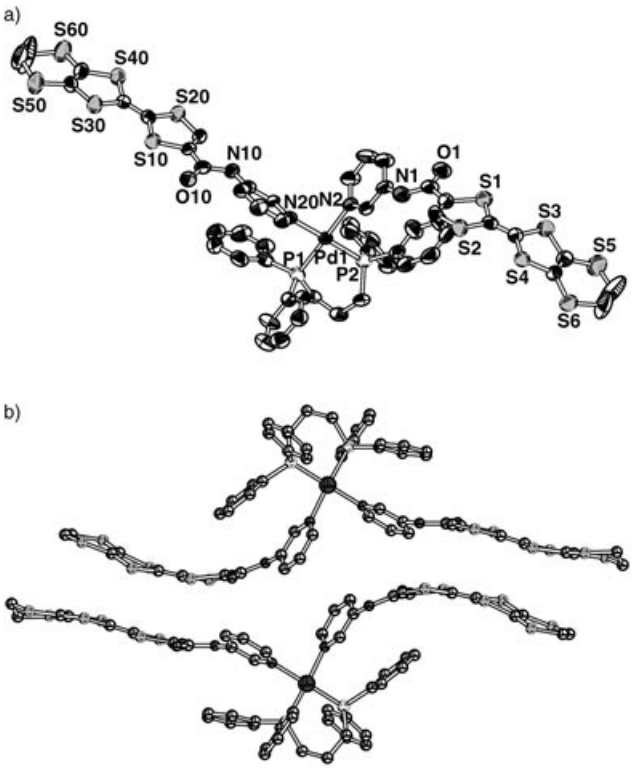

Figure 7. a) ORTEP view of the $[Pd(dppp)(\mathbf{2a})_2]^{2+}$ unit in $[Pd(dppp)(\mathbf{2a})_2](OTf)_2 \cdot CHCl_3 \cdot Et_2O$, with 50% probability displacement ellipsoids; b) *dl* pair of enantiomers of $[Pd(dppp)(\mathbf{2a})_2]^{2+}$.

As expected, besides the chelating diphosphine, the square planar palladium center is *cis* coordinated by two TTF-amido-pyridines **2a**, whose conformations are highly distorted mainly about the NH–Py bond, as shown by the following set of dihedral angles: for ligand A $\phi = 69.3(2)°$, $\theta_1 = 15.9(9)°$, $\theta_2 = 10.7(10)°$, $\theta_3 = 44.4(12)°$ and for ligand B $\phi = 35.1(2)°$, $\theta_1 = 8.8(8)°$, $\theta_2 = 1.5(10)°$, $\theta_3 = 32.5(10)°$. Selected bond lengths and angles concerning the TTF moiety are listed in Table 1, whereas those related to the coordination sphere of palladium are given in Table 4. These parameters have usual values and compare with those already described in the literature.[30–32,34]

Table 4. Selected bond lengths [Å] and angles [°] for $[Pd(dppp)(\mathbf{2a})_2](OTf)_2 \cdot CHCl_3 \cdot Et_2O$.

Pd1–N20	2.106(6)	Pd1–P1	2.280(2)
Pd1–N2	2.124(5)	Pd1–P2	2.262(2)
N20-Pd1-N2	86.7(2)	N20-Pd1-P1	91.02(15)
N20-Pd1-P2	179.11(16)	N2-Pd1-P1	177.66(17)
N2-Pd1-P2	94.15(17)	P2-Pd1-P1	88.15(7)

The conformation of the complex is of *anti* type, the centrosymmetric dimers observed within the structure correspond to the *dl* racemic pairs of enantiomers. The two TTF cores are arranged, somewhat surprisingly, in an antiparallel manner, yielding a dihedral angle of practically 180° in between. The triflate anions are engaged in hydrogen bonds of N–H··· O (OTf), C–H···O (OTf) and C_{Py}–H···O (OTf) type (Table 2) with both TTF-amido-pyridines, thus preventing the formation of an extended hydrogen-bond network. Recently, Stang and co-workers tried to rationalize[28] the crystalline structures of a large series of metal complexes containing *p*-benzoylamidopyridine as ligand through the competition between the different directional interactions involved, such as coordination, hydrogen bonding and π–π stacking. In our case, additional intermolecular van der Waals S···S interactions, specific to sulfur-rich compounds, are present. Within a centrosymmetric *dl* pair of complexes, represented in Figure 7b, several short intermolecular S···S contacts are observed, with values ranging between 3.596(3) Å and 3.776(3) Å. Since the intermolecular S···S distances between these centrosymmetric dyads are quite longer, they are considered as isolated in the solid. A very similar structure was observed for the complex with dppe (bis(diphenylphosphino)ethane) instead of dppp, synthesized by mixing the precursor $[Pd(dppe)(OTf)_2]$, obtained by chlorine abstraction from $[PdCl_2(dppe)]$, with **2a**. Nevertheless, this structure will not be discussed hereafter, since its quality, due to the small size of the single crystals, was too poor. However, this type of arrangement of dicationic complexes in centrosymmetric dyads seems to be recurrent and favored by two factors: the conformational chirality on one hand and S···S intermolecular contacts on the other. The question arises whether the same pattern would be observed in radical cation salts of the complexes, eventually with enhanced interactions between the dyads. Cyclic voltammetry measurements indicated the same oxidation potentials as for uncoordinated ligands and showed no split of the redox waves. These square-planar complexes are currently being explored in electrocrystallization experiments and the results of these investigations will be reported in due course.

Conclusion

A series of six TTF-amidopyridine and -2,2′-bipyridine derivatives has been synthesized, and their crystal structures have been analyzed with respect to the ability of the hydrogen-bond donor/acceptor character of the amide and pyridine groups to compete with π–π intermolecular interactions and S···S van der Waals interactions, and to direct the pattern of intermolecular association in the solid state. Electrochemical studies on these donors showed that they are all good precursors for the synthesis of radical cation salts. Single crystals of one such salt, namely $[\mathbf{2a}]^{\cdot+}PF_6^-$, were prepared by electrocrystallization. The analysis of the structure, combined with that of $\beta_{HOMO-HOMO}$ interaction obtained by extended Hückel calculations, showed that the radical cations form strong dimers, and because of the presence of a THF solvent molecule playing the role of a hydrogen bond acceptor, no extended hydrogen-bond network was formed at the supramolecular level. Finally we synthesized square-planar complexes of Pd^{2+} and Pt^{2+}, coordinated by a chelating diphosphine, such dppp or dppe, and two redox active donors **2a**. The Pd complexes have fluxional conformations at room temperature, due to the rotation of pyridine ligands about the Pd–N bond, whereas the Pt counterparts exist as a mixture of *meso* and racemic *dl* conformations, as demonstrated by ^{31}P NMR spectroscopy. In the solid state, the complex $[Pd(dppp)(\mathbf{2a})_2]$ is stabilized as *dl* racemic conformers, whose TTF cores are arranged in an antiparallel manner. Cyclic voltammetry experiments demonstrate that oxidation of complexes occurs at the same potentials as that of free ligands.

Experimental Section

General comments: Dry CH_2Cl_2, $CHCl_3$ and MeCN were obtained by distillation over P_2O_5, and THF was distilled over sodium and benzophenone. Nuclear magnetic resonance spectra were recorded for compounds **2a**, **2b**, **3**, on a Bruker Avance ARX 400 spectrometer operating at 400.13 MHz for ^1H and 100.62 MHz for ^{13}C and for compounds **5**, **6**, **7**, Pd and Pt complexes on a Bruker Avance DRX 500 spectrometer operating at 500.04 MHz for ^1H, 125.75 MHz for ^{13}C and 202.39 MHz for ^{31}P. Chemical shifts are expressed in parts per million (ppm) downfield from external TMS. The following abbreviations are used: s, singlet; d, doublet; t, triplet; m, multiplet; br, broad. Mass spectrometry was performed for compounds **2a** and **2b** on a HP 5989A spectrometer in the EI mode, with an ionization energy of 70 eV, and for all the other compounds on a Jeol JMS 700 B/ES spectrometer in electrospray mode. Elemental analyses were performed by the "Service d'Analyse du CNRS" at Gif/Yvette, France.

4,5-Ethylenedithio-4′-*meta*-pyridylcarbamoyltetrathiafulvalene (2a): Compound **1** (0.53 g, 1.48 mmol) in THF (30 mL) was added dropwise to a solution of 3-aminopyridine (0.68 g, 7.23 mmol) in THF (15 mL), under magnetic stirring. The solution became clear and a red precipitate was

formed. After 4 h of stirring at room temperature, the solvent was evaporated, and the red solid was suspended in water (150 mL), filtered, washed with diethyl ether (40 mL), and dissolved in hot THF (100 mL). Compound **2a** was recovered as red crystals, suitable for a single-crystal X-ray analysis, after filtration and recrystallization in THF or MeCN. Yield: 0.4 g (65%); ^{1}H NMR ([D6]DMSO): $\delta = 10.50$ (s, 1H; NH), 8.78 (d, $J = 2.4$ Hz, 1H; H_a), 8.33 (dd, $J^1 = 4.7$ Hz, $J^2 = 1.2$ Hz, 1H; H_b), 8.03 (m, 1H; H_c), 7.89 (s, 1H; CH), 7.39 (dd, $J^1 = 8.3$ Hz, $J^2 = 4.7$ Hz, 1H; H_d), 3.42 ppm (s, 4H; CH_2CH_2); ^{13}C NMR ([D6]DMSO): $\delta = 157.9$ (C=O), 152.9 (HC–N_{py}), 149.3 (HC–N_{py}), 146.4 (C_{py}–NH), 140.0 (HC_{py}), 128.9 (HC_{py}), 132.4 (C-CO), 125.8 (=CH), 113.2 (C=C), 112.7 (C=C), 106.2 (C=C), 31.4 ppm (CH_2CH_2); MS (EI): *m/z* (%): 414 (100) [M^+], 386 (57) [$M^+ - CH_2CH_2$], 310 (22) [$M^+ - CSCH_2CH_2S$]; m.p. 210°C (decomp); elemental analysis calcd (%) for $(C_{14}H_{10}N_2OS_6)_2 \cdot$THF (901.4): C 42.64, H 3.13, N 6.21; found: C 42.13, H 3.06, N 6.54.

4,5-Ethylenedithio-4′-*para*-pyridylcarbamoyltetrathiafulvalene (2b): This compound was synthesized by a similar procedure to that used for **2a** starting from 4-aminopyridine (0.66 g, 7.02 mmol) and **1** (0.53 g, 1.48 mmol). After recrystallization in acetonitrile, **2b** was recovered as crystalline red platelets, suitable for a X-ray diffraction analysis. Yield: 0.47 g (77%); ^{1}H NMR ([D6]DMSO): $\delta = 10.61$ (s, 1H; NH), 8.46 (d, $J = 2.5$ Hz, 2H; H_a), 7.94 (s, 1H; CH), 7.61 (d, $J = 2.5$ Hz, 2H; H_b), 3.40 ppm (s, 4H; CH_2CH_2); ^{13}C NMR ([D6]DMSO): $\delta = 158.4$ (C=O), 150.9 (HC–N_{py}), 145.4 (C_{py}–NH), 133.3 (C–CO), 128.8 (=CH), 115.6 (C=C), 114.3 (HC_{py}), 113.7 (C=C), 113.4 (C=C), 105.3 (C=C), 30.1 ppm (CH_2CH_2); MS (EI): *m/z* (%): 414 (100) [M^+], 294 (6) [M^+–CONHPy]; m.p. 225°C (decomp); elemental analysis calcd (%) for $C_{14}H_{10}N_2OS_6$ (414.6): C 40.55, H 2.43, N 6.76; found: C 40.55, H 2.56, N 6.82.

4,5-Ethylenedithio-4′-*meta*-2,2′-bipyridylcarbamoyltetrathiafulvalene (3): 5-Amino-2,2′-bipyridine (0.27 g, 1.58 mmol) was dissolved in THF (30 mL) containing NEt_3 (1 mL); then a solution of **1** (0.50 g, 1.4 mmol) in THF (30 mL) was added dropwise. The solution turned red upon this addition. The solvent was evaporated after 3 h of stirring at room temperature, and the resulting solid was suspended in water, filtered, washed with a saturated solution of $NaHCO_3$ (40 mL), then with diethyl ether (40 mL), and dried under vacuum. The orange powder thus obtained was purified by a Soxhlet extraction with THF (60 mL) for a period of 48 h. Evaporation of solvent yielded **3** as a bright red solid. Yield 0.36 g (52%). Suitable crystals for an X-ray analysis were grown by slow diffusion of methanol into a solution of **3** in dimethylsulfoxide. ^{1}H NMR ([D6]DMSO): $\delta = 10.68$ (brs, 1H; NH), 8.93 (s, 1H; H_a), 8.69 (brs, 1H; H_b), 8.39 (m, 2H; H_c), 8.23 (d, $J = 7.8$ Hz, 1H; H_d), 7.95 (brs, 2H; CH and H_e), 7.45 (brs, 1H; H_f), 3.44 ppm (s, 4H; CH_2CH_2); ^{13}C NMR ([D6]DMSO): $\delta = 158.5$ (C=O), 155.7, 151.5, 150.0, 141.8, 138.1, 136.2, 128.7, 121.4, 121.4, 120.9 (C_{Py}), 133.9 (C–CO), 124.6 (=CH), 114.0, 113.7, 105.4 (C=C), 30.4 ppm (CH_2CH_2); MS (electrospray): *m/z* (%): 491 (50) [M^+], 463 (100) [$M^+ - CH_2CH_2$]; m.p. 166°C (decomp); elemental analysis calcd (%) for $C_{19}H_{13}N_3OS_6$ (491.7): C 46.44, H 2.65, N 8.55; found: C 45.78, H 2.59, N 8.29.

4,5-Bis(thiomethyl)-4′-*meta*-pyridylcarbamoyltetrathiafulvalene (5): Compound **4** (0.50 g, 1.39 mmol), which was prepared by a similar procedure with that for **1**, dissolved in THF (15 mL) was added dropwise to a solution of 3-aminopyridine (0.65 g, 6.9 mmol) in THF (15 mL), under magnetic stirring. The solution became clear and was allowed to stir at room temperature for 3 h. After filtration, the solvent was removed under vacuum and the red solid thus obtained was dissolved in CH_2Cl_2 (ca. 100 mL); the resulting solution was washed with water, dried over $MgSO_4$, and filtered. Finally, evaporation of solvent and recrystallization in CH_2Cl_2 yielded **5** as orange crystalline platelets, suitable for an X-ray analysis. Yield: 0.51 g (88%); ^{1}H NMR ([D6]DMSO): $\delta = 10.49$ (s, 1H; NH), 8.75 (d, $J = 2.4$ Hz, 1H; H_a), 8.30 (dd, $J^1 = 4.7$ Hz, $J^2 = 1.3$ Hz, 1H; H_b), 8.01 (ddd, $J^1 = 8.3$ Hz, $J^2 = J^3 = 2.2$ Hz, 1H; H_c), 7.86 (s, 1H; CH), 7.37 (dd, $J^1 = 8.3$ Hz, $J^2 = 4.7$ Hz, 1H; H_d), 2.43 ppm (s, 6H; CH_3); ^{13}C NMR ([D6]DMSO): $\delta = 157.9$ (C=O), 141.2, 135.2, (HC_{Py}), 144.8 (C_{Py}–NH), 126.9, 126.4 (HC_{Py}), 133.0 (C–CO), 124.2 (=CH), 113.0, 106.9 (C=C), 18.7 ppm (SCH_3); MS (electrospray): *m/z* (%): 416 (100) [M^+], 401 (10) [$M^+ - CH_3$]; m.p. 183°C (decomp); elemental analysis calcd (%) for $C_{14}H_{12}N_2OS_6 \cdot CH_2Cl_2$ (501.6): C 36.51, H 2.78, N 5.80; found: C 35.92, H 2.81, N 5.88.

4,5-Bis(thiomethyl)-4′-*meta*-2,2′-bipyridylcarbamoyltetrathiafulvalene (6): 5-Amino-2,2′-bipyridine (0.12 g, 0.71 mmol) was dissolved in THF (10 mL) containing NEt_3 (1 mL); then a solution of **4** (0.26 g, 0.71 mmol) in THF (15 mL) was added dropwise. A red precipitate appeared upon addition. The mixture was stirred at 50°C for 5 h, then, after evaporation of solvent, a violet solid was obtained. This solid was suspended in solution 1 M KOH (80 mL), concomitantly the color changed to orange, and then the compound was extracted with CH_2Cl_2. After evaporation of solvent and recrystallization in a THF/CH_2Cl_2 1:1 mixture, **6** was recovered as orange crystalline needles. Yield: 0.25 g (72%). Single crystals for X-ray analysis were grown by slow diffusion of methanol into a solution of **6** in dimethylsulfoxide. ^{1}H NMR ([D6]DMSO): $\delta = 10.66$ (brs, 1H; NH), 8.84 (d, $J = 1.9$ Hz, 1H; H_a), 8.64 (d, $J = 4{,}3$ Hz, 1H; H_b), 8.32 (m, 2H; H_c), 8.18 (dd, $J^1 = 8.6$ Hz, $J^2 = 2.4$ Hz, 1H; H_d), 7.90 (dd, $J^1 = J^2 = 7.8$ Hz, 1H; H_e), 7.82 (s, 1H; CH), 7.39 (dd, $J^1 = 7.4$ Hz, $J^2 = 5$ Hz, 1H; H_f), 2.44 ppm (s, 6H; CH_3); ^{13}C NMR ([D6]DMSO): $\delta = 157.8$ (C=O), 154.8, 150.7, 149.3, 141.1, 137.5, 135.5, 128.0, 126.4, 120.4, 120.2 (C_{Py}), 133.9 (C–CO), 124.6 (=CH), 114.0, 113.7, 105.4 (C=C), 30.4 ppm (CH_2CH_2); MS (electrospray): *m/z* (%): 493 (100) [M^+], 478 (40) [$M^+ - CH_3$], 464 (12) [$M^+ - 2CH_3$]; m.p. 224°C (decomp); elemental analysis calcd (%) for $C_{19}H_{15}N_3OS_6$ (493.7): C 46.22, H 3.06, N 8.51; found: C 46.11, H 3.04, N 7.94.

5,5′-Bis(4,5-bis(thiomethyl)-4′-carbamoyltetrathiafulvalene)-2,2′-bipyridine (7): 5,5′-Diamino-2,2′-bipyridine (0.11 g, 0.58 mmol) dissolved in THF (10 mL) was added to a solution of **4** (0.42 g, 1.17 mmol) in THF (40 mL) and NEt_3 (2 mL). Within a few minutes the solution became clear and a red precipitate appeared. The reaction mixture was allowed to stir at room temperature overnight, and then it was heated at 60°C for 48 h. After complete evaporation of the solvent, the resulting red residue was washed once with an aqueous NaOH solution (10^{-2} M, 40 mL) and once with diethyl ether (40 mL), and was then recrystallized in pyridine. Bright orange needles of **7** were obtained after filtration and drying. Yield: 0.42 g (74%). Suitable crystals for X-ray analysis were grown by slow diffusion of diethyl ether into a solution of **7** in pyridine or in dimethylformamide. For the latter, two polymorphs containing DMF crystallized, none of them isostructural with the one described in this paper. ^{1}H NMR ([D5]Py, 40°C): $\delta = 11.10$ (s, 2H; NH), 9.15 (s, 2H; H_a), 8.61 (d, $J = 8.7$ Hz, 2H; H_b), 8.39 (d, $J = 8.7$ Hz 2H; H_c), 7.84 (s, 2H; CH), 2.38 (s, 6H; CH_3), 2.35 ppm (s, 6H; CH_3); ^{13}C NMR ([D_7]DMF, 80°C): $\delta = 158.3$ (C=O), 151.5, 150.0, 141.5, 135.7, 128.1, 127.4, 120.4 (C_{Py}), 134.1 (C–CO), 123.9 (=CH), 114.0, 113.7, 105.4 (C=C), 30.4 ppm (CH_2CH_2); MS (electrospray): *m/z* (%): 830 (100) [M^+]; m.p. 280°C (decomp); elemental analysis calcd (%) for $C_{28}H_{22}N_4O_2S_{12} \cdot 2$Py (989.5): C 46.13, H 3.26, N 8.49; found: C 45.92, H 3.18, N 8.60.

[Pd(dppp)(2a)$_2$](OTf)$_2$: [Pd(dppp)(OTf)$_2$] (0.084 g, 0.1 mmol) dissolved in THF (13 mL) was added under argon to a solution of **2a** (0.091 g, 0.2 mmol) in THF (50 mL) in a Schlenk tube. The resulting mixture was stirred at room temperature for 48 h. The complex was recovered as red platelets by layering diethyl ether onto a solution of the complex in THF/$CHCl_3$ 1:1. Yield: 0.13 g, (77%); ^{1}H NMR (CD_3CN): $\delta = 8.94$ (brs, 2H; H_a), 8.66 (brs, 2H; NH), 8.28 (brs, 2H; H_b), 7.67 (brs, 2H; H_c), 7.49 (m, 12H; Ph), 7.34 (brs, 8H; Ph), 7.19 (brs, 2H; H_d), 3.41 (s, 8H; CH_2CH_2), 2.98 (brs, 4H; PCH_2), 2.21 ppm (m, 2H; CH_2); ^{31}P NMR (CD_3CN): $\delta = 2.7$ ppm (s); MS (electrospray): *m/z* (%): 1496.7 (100) [$M^+ - OTf$].

[Pt(dppp)(2a)$_2$](OTf)$_2$: This complex was obtained, as a red brown powder, by a similar procedure to that used for the Pd complex, starting from **2a** (0.13 g, 0.29 mmol) and [Pt(dppp)(OTf)$_2$] (0.09 g, 0.1 mmol). Yield: 0.088 g (51%); ^{31}P NMR (CH_2Cl_2): $\delta = -10.4$ (s, A), -11.3 ppm (s, B); ratio A/B = 1:1.6; MS (electrospray): *m/z* (%): 1584.9 (100) [$M^+ - OTf$].

[Pd(dppe)(2a)$_2$](OTf)$_2$: [Pd(dppe)(OTf)$_2$] (0.049 g, 0.06 mmol) dissolved in $CHCl_3$ (10 mL) was added under argon to a solution of **2a** (0.051 g, 0.12 mmol) in $CHCl_3$ (50 mL) in a Schlenk tube. After 3 h of stirring at room temperature the solution was concentrated to 5 mL, and the complex was isolated by filtration. Yield: 0.07 g (70%). Single crystals for X-ray analysis were grown by slow evaporation of a solution of complex in $CHCl_3$. ^{31}P NMR ($CHCl_3$): $\delta = 65.2$ ppm (s).

X-ray crystallography: Details about data collection and solution refinement are given in Table 5. Data were collected on a Stoe-IPDS imaging plate system for all the compounds. Structures were solved by direct methods (SHELXS) and refined (SHELXL-97)[37] by full-matrix least-

Table 5. X-ray crystallographic data.

	2a·0.5 MeCN	**2b**	**3**	**5**·CH_2Cl_2
formula	$C_{15}H_{11.5}N_{2.5}OS_6$	$C_{14}H_{10}N_2OS_6$	$C_{19}H_{13}N_3OS_6$	$C_{15}H_{14}C_{l2}N_2OS_6$
M_r	435.13	414.6	491.68	501.54
T [K]	293(2)	293(2)	293(2)	293(2)
crystal system	orthorhombic	monoclinic	monoclinic	monoclinic
space group	*Pbca*	$P2_1/c$	$P2_1/n$	$P2_1/n$
a [Å]	13.1017(7)	18.8729(12)	16.8130(16)	6.2167(5)
b [Å]	11.5553(10)	7.188(5)	7.9070(7)	32.827(2)
c [Å]	24.450(2)	12.393(7)	16.8200(18)	10.6035(8)
β [°]		104.133(7)	107.535(11)	97.756(9)
V [Å^3]	3701.5(5)	1630.3(15)	2132.2(4)	2144.1(3)
Z	8	4	4	4
ρ_{calcd} [g cm^{-3}]	1.562	1.689	1.532	1.554
μ [mm^{-1}]	0.746	0.842	0.658	0.896
F(000)	1784	848	1008	1024
crystal size [mm]	0.27 × 0.20 × 0.18	0.27 × 0.15 × 0.03	0.46 × 0.15 × 0.06	0.84 × 0.15 × 0.08
θ range [°]	2.28–25.95	2.23–25.84	2.54–25.92	2.04–25.79
reflections collected	30062	16281	17745	13061
independent reflections	3592	3122	3897	3823
R_{int}	0.0649	0.1139	0.0715	0.1427
parameters	222	208	262	235
GOF on F^2	0.881	0.862	0.544	0.801
$R1$[a] $[I > 2\sigma(I)]$/$wR2$[b]	0.0373/0.0792	0.0452/0.0873	0.0356/0.0619	0.0557/0.1340
largest diff. peak/hole [e Å^{-3}]	0.410/−0.354	0.507/−0.290	0.234/−0.219	0.386/−0.345

	6·MeOH	**7**·2 Py	(**2a**)PF_6·THF	[Pd(dppp)(**2a**)$_2$]-(OTf)$_2$·$CHCl_3$·Et_2O
formula	$C_{20}H_{18}N_3O_2S_6$	$C_{19}H_{16}N_3OS_6$	$C_{18}H_{18}F_6N_2O_2PS_6$	$C_{62}H_{57}Cl_3F_6N_4O_9P_2PdS_{14}$
M_r	524.73	494.71	631.67	1839.65
T [K]	200(2)	230(2)	293(2)	200(2)
crystal system	triclinic	monoclinic	triclinic	triclinic
Space group	$P\bar{1}$	$P2_1/c$	$P\bar{1}$	$P\bar{1}$
a [Å]	9.3028(12)	5.5486(5)	9.3603(19)	13.403(2)
b [Å]	10.4217(16)	17.7184(17)	9.762(2)	15.536(3)
c [Å]	12.5027(18)	22.091(2)	14.545(3)	19.336(3)
α [°]	86.383(18)		108.11(3)	100.308(17)
β [°]	74.479(16)	92.050(11)	99.72(3)	100.840(17)
γ [°]	81.720(17)		90.98(3)	99.066(19)
V [Å^3]	1155.4(3)	2170.4(4)	1241.7(4)	3813.5(10)
Z	2	4	2	2
ρ_{calcd} [g cm^{-3}]	1.508	1.514	1.689	1.602
μ [mm^{-1}]	0.616	0.647	0.682	0.844
F(000)	542	1020	642	1868
crystal size [mm]	0.6 × 0.58 × 0.38	0.54 × 0.05 × 0.04	0.38 × 0.19 × 0.09	0.23 × 0.17 × 0.12
θ range [°]	1.98–25.98	2.17–25.87	2.20–26.00	1.87–25.96
reflections collected	11817	21466	12569	37404
independent reflections	4195	4166	4476	13527
R_{int}	0.0478	0.1041	0.1023	0.0749
parameters	282	0.264	316	887
GOF on F^2	0.924	0.540	0.834	0.835
$R1$[a] $[I > 2\sigma(I)]$/$wR2$[b]	0.0298/0.0693	0.0394/0.0628	0.0614/0.1539	0.0624/0.1426
largest diff. peak/hole [e Å^{-3}]	0.355/-0.218	0.273/−0.220	0.569/−0.346	1.185/−0.576

squares methods. Hydrogen atoms were introduced at calculated positions (riding model), included in structure factor calculations, and not refined. All the heavy atoms were refined anisotropically. CCDC-225225 (**2a**), CCDC-225226 (**2b**), CCDC-225227 (**3**), CCDC-225233 (**4′**), CCDC-225228 (**5**), CCDC-225229 (**6**), CCDC-225230 (**7**), CCDC-225231 ((**2a**)PF_6·THF), CCDC-225232 ([Pd(dppp)(**2a**)$_2$](OTf)$_2$·$CHCl_3$·Et_2O) contain the supplementary crystallographic data for this paper. These data can be obtained free of charge via www.ccdc.cam.uk/conts/retrieving.html (or from the Cambridge Crystallographic Data Centre, 12 Union Road, Cambridge CB21EZ, UK; fax: (+44) 1223–336–033; or deposit@ccdc.cam.uk).

Theoretical calculations: The overlap interaction energies ($\beta_{HOMO-HOMO}$) were of the extended Hückel type.[38] A modified Wollsberg–Helmholtz formula was used to calculate the non-diagonal $H_{\mu\nu}$ values.[39] Double-ζ orbitals for C, S, N and O were used.

Acknowledgement

Financial support from CNRS (Centre National de la Recherche Scientifique), the Ministère de l'Education et de la Recherche (grant for T.D.) and University of Angers is gratefully acknowledged. The authors thank Dr. D. Rondeau (University of Angers) for electrospray mass spectra measurements and Prof. C. Janiak (University of Freiburg, Germany) for helpful discussions concerning the synthesis of 5,5′-diamino-2,2′-bipyridine.

[1] a) G. Li, Y. Song, H. Hou, L. Li, Y. Fan, Y. Zhu, X. Meng, L. Mi, *Inorg. Chem.* **2003**, *42*, 913–920; b) E. Lindner, R. Zong, K. Eichele, U. Weisser, M. Ströbele, *Eur. J. Inorg. Chem.* **2003**, 705–712.

[2] a) M. Buda, J.-C. Moutet, E. Saint-Aman, A. De Cian, J. Fischer, R. Ziessel, *Inorg. Chem.* **1998**, *37*, 4146–4148; b) A. Ion, J.-C. Moutet, E. Saint-Aman, G. Royal, S. Tingry, J. Pecaut, S. Menage, R. Ziessel, *Inorg. Chem.* **2001**, *40*, 3632–3636; c) A. Ion, M. Buda, J.-C. Moutet, E. Saint-Aman, G. Royal, I. Gautier-Luneau, M. Bonin, R. Ziessel, *Eur. J. Inorg. Chem.* **2002**, 1357–1366.

[3] U. Siemeling, J. Vor der Brüggen, U. Vorfeld, B. Neumann, A. Stammler, H.-G. Stammler, A. Brockhinke, R. Plessow, P. Zanello, F. Laschi, F. Fabrizi de Biani, M. Fontani, S. Steenken, M. Stapper, G. Gurzadyan, *Chem. Eur. J.* **2003**, *9*, 2819–2833.

[4] a) J. M. Williams, J. R. Ferraro, R. J. Thorn, K. D. Carlson, U. Geiser, H. H. Wang, A. M. Kini, M.-H. Whangbo, *Organic Superconductors (Including Fullerenes), Synthesis, Structure, Properties and Theory*, Prentice Hall **1992**; b) M. R. Bryce, *J. Mater. Chem.* **1995**, *5*, 1469–1753; c) J. L. Segura, N. Martin, *Angew. Chem.* **2001**, *113*, 1416–1455; *Angew. Chem. Int. Ed.* **2001**, *40*, 1372–1409.

[5] a) H. Tanaka, Y. Okano, H. Kobayashi, W. Suzuki, A. Kobayashi, *Science* **2001**, *291*, 285–287; b) C. Rovira, J. J. Novoa, J.-L. Mozos, P. Ordejon, E. Canadell, *Phys. Rev. B* **2002**, *65*, 081104.

[6] a) M. Kurmoo, A. W. Graham, P. Day, S. J. Coles, M. B. Hurthouse, J. L. Caulfield, J. Singleton, F. L. Pratt, W. Hayes, L. Ducasse, P. Guinneau, *J. Am. Chem. Soc.* **1995**, *117*, 12209–12217; b) E. Coronado, J. R. Galan-Mascaros, C. J. Gomez-Garcia, V. Laukhin, *Nature* **2000**, *408*, 447–449.

[7] M. Mas-Torrent, S. S. Turner, K. Wurst, J. Vidal-Gancedo, X. Ribas, J. Veciana, P. Day, C. Rovira, *Inorg. Chem.* **2003**, *42*, 7544–7549.

[8] F. Le Derf, M. Mazari, N. Mercier, E. Levillain, G. Trippé, A. Riou, P. Richomme, J. Becher, J. Garin, J. Orduna, N. Gallego-Planas, A. Gorgues, M. Sallé, *Chem. Eur. J.* **2001**, *7*, 447–455.

[9] a) M. Munakata, T. Kuroda-Sawa, M. Maekawa, A. Hirota, S. Kitagawa, *Inorg. Chem.* **1995**, *34*, 2705–2710; b) J. C. Zhong, Y. Misaki, M. Munakata, T. Kuroda-Sawa, M. Maekawa, Y. Suenaga, H. Konaka, *Inorg. Chem.* **2001**, *40*, 7096–7098; c) J. Ramos, V. M. Yartsev, S. Golhen, L. Ouahab, P. Delhaès, *J. Mater. Chem.* **1997**, *7*, 1313–1319.

[10] a) M. Fourmigué, P. Batail, *Bull. Soc. Chim. Fr.* **1992**, *129*, 29–36; b) M. Fourmigué, C. E. Uzelmeier, K. Boubekeur, S. L. Bartley, K. R. Dunbar, *J. Organomet. Chem.* **1997**, *529*, 343–350; c) E. Cerrada, C. Diaz, M. C. Diaz, M. B. Hursthouse, M. Laguna, M. E. Light, *J. Chem. Soc. Dalton Trans.* **2002**, 1104–1109; d) N. Avarvari, D. Martin, M. Fourmigué, *J. Organomet. Chem.* **2002**, *643/644*, 292–300.

[11] S. S. Kuduva, N. Avarvari, M. Fourmigué *J. Chem. Soc. Dalton Trans.* **2002**, 3686–3690.

[12] a) W. Xu, D. Zhang, H. Li, D. Zhu, *J. Mater. Chem.* **1999**, *9*, 1245–1249; b) L. M. Goldenberg, J. Y. Becker, O. P.-T. Levi, V. Y. Khodorkovsky, M. R. Bryce, M. C. Petty, *J. Chem. Soc. Chem. Commun.* **1995**, 475–476; c) O. P.-T. Levi, J. Y. Becker, A. Ellern, V. Y. Khodorkovsky, *Tetrahedron Lett.* **2001**, *42*, 1571–1573; d) J.-P. Griffiths, R. J. Brown, P. Day, C. J. Matthews, B. Vital, J. D. Wallis, *Tetrahedron Lett.* **2003**, *44*, 3127–3131; e) C. Jia, D. Zhang, Y. Xu, W. Xu, H. Hu, D. Zhu, *Synth. Met.* **2003**, *132*, 249–255.

[13] a) M. Iyoda, Y. Kuwatani, N. Ueno, M. Oda, *J. Chem. Soc. Chem. Commun.* **1992**, 158–159; b) A. J. Moore, A. S. Batsanov, M. R. Bryce, J. A. K. Howard, V. Khodorkovsky, L. Shapiro, A. Shames, *Eur. J. Org. Chem.* **2001**, 73–78.

[14] R. Andreu, I. Malfant, P. G. Lacroix, P. Cassoux, *Eur. J. Org. Chem.* **2000**, 737–741.

[15] S.-X. Liu, S. Dolder, M. Pilkington, S. Decurtins, *J. Org. Chem.* **2002**, *67*, 3160–3162.

[16] a) S. Campagna, S. Serroni, F. Puntoriero, F. Loiseau, L. De Cola, C. J. Kleverlaan, J. Becher, A. P. Sorensen, P. Hascoat, N. Thorup, *Chem. Eur. J.* **2002**, *8*, 4461–4469; b) S. Bouguessa, K. Hervé, S. Golhen, L. Ouahab, J.-M. Fabre, *New J. Chem.* **2003**, *27*, 560–564; c) S.-X. Liu, S. Dolder, E. B. Rusanov, H. Stoeckli-Evans, S. Decurtins, *C. R. Acad. Sci. Chimie* **2003**, *6*, 657–662.

[17] a) F. Iwahori, S. Golhen, L. Ouahab, R. Carlier, J.-P. Sutter, *Inorg. Chem.* **2001**, *40*, 6541–6542; b) L. Ouahab, F. Iwahori, S. Golhen, R. Carlier, J.-P. Sutter, *Synth. Met.* **2003**, *133–134*, 505–507; c) S.-X. Liu, S. Dolder, P. Franz, A. Neels, H. Stoeckli-Evans, S. Decurtins, *Inorg. Chem.* **2003**, *42*, 4801–4803.

[18] F. Setifi, L. Ouahab, S. Golhen, Y. Yoshida, G. Saito, *Inorg. Chem.* **2003**, *42*, 1791–1793.

[19] a) L. Leiserowitz, A. T. Hagler, *Proc. R. Soc. London A* **1983**, *388*, 133; b) G. Tayhas, R. Palmore, J. C. McDonald, *The Amide Linkage: Selected Structural Aspects in Chemistry, Biochemistry and Materials Science*, Wiley, **2000**, pp. 291–336.

[20] K. Heuzé, M. Fourmigué, P. Batail, *J. Mater. Chem.* **1999**, *9*, 2373–2379.

[21] S. A. Baudron, N. Avarvari, P. Batail, C. Coulon, R. Clérac, E. Canadell, P. Auban-Senzier, *J. Am. Chem. Soc.* **2003**, *125*, 11583–11590.

[22] K. Heuzé, M. Fourmigué, P. Batail, E. Canadell, P. Auban-Senzier, *Chem. Eur. J.* **1999**, *5*, 2971–2976.

[23] S. A. Baudron, P. Batail, C. Rovira, E. Canadell, R. Clérac, *Chem. Commun.* **2003**, 1820–1821.

[24] A. S. F. Boyd, G. Cooke, F. M. A. Duclairoir, V. M. Rotello, *Tetrahedron Lett.* **2003**, *44*, 303–306.

[25] a) K. Heuzé, C. Mézière, M. Fourmigué, P. Batail, C. Coulon, E. Canadell, P. Auban-Senzier, D. Jérome, *Chem. Mater.* **2000**, *12*, 1898–1904; b) K. Heuzé, M. Fourmigué, P. Batail, C. Coulon, R. Clérac, E. Canadell, P. Auban-Senzier, S. Ravy, D. Jérome, *Adv. Mater.* **2003**, *15*, 1251–1254.

[26] B. Zhang, R. Breslow, *J. Am. Chem. Soc.* **1997**, *119*, 1676–1681.

[27] M. Etter, *Acc. Chem. Res.* **1990**, *23*, 120–126.

[28] J. C. Noveron, M. S. Lah, R. E. Del Sesto, A. M. Arif, J. S. Miller, P. J. Stang, *J. Am. Chem. Soc.* **2002**, *124*, 6613–6625.

[29] C. Janiak, S. Deblon, H.-P. Wu, M. J. Kolm, P. Klüfers, H. Piotrowski, P. Mayer, *Eur. J. Inorg. Chem.* **1999**, 1507–1521.

[30] a) P. J. Stang, D. H. Chao, *J. Am. Chem. Soc.* **1994**, *116*, 4981–4982; b) P. J. Stang, D. H. Chao, S. Saito, A. M. Arif, *J. Am. Chem. Soc.* **1995**, *117*, 6273–6283.

[31] S. S. Sun, J. A. Anspach, A. J. Lees, P. Y. Zavalij, *Organometallics* **2002**, *21*, 685–693.

[32] P. J. Stang, D. H. Chao, K. Chen, G. M. Gray, D. C. Muddiman, R. D. Smith, *J. Am. Chem. Soc.* **1997**, *119*, 5163–5168.

[33] a) B. Olenyuk, J. A. Whiteford, P. J. Stang, *J. Am. Chem. Soc.* **1996**, *118*, 8221–8230; b) C. Müller, J. A. Whiteford, P. J. Stang, *J. Am. Chem. Soc.* **1998**, *120*, 9827–9837.

[34] a) P. J. Stang, J. Fan, B. Olenyuk, *Chem. Commun.* **1997**, 1453–1454; b) J. Fan, J. A. Whiteford, B. Olenyuk, M. D. Levin, P. J. Stang, E. B. Fleischer, *J. Am. Chem. Soc.* **1999**, *121*, 2741–2752; c) T. Habicher, J.-F. Nierengarten, V. Gramlich, F. Diederich, *Angew. Chem.* **1998**, *110*, 2019–2022; *Angew. Chem. Int. Ed. Engl.* **1998**, *37*, 1916–1919; ; d) F. Würthner, A. Sautter, D. Schmid, P. J. A. Weber, *Chem. Eur. J.* **2001**, *7*, 894–902.

[35] T. G. Appleton, M. A. Bennett, I. B. Tomkins, *J. Chem. Soc. Dalton Trans.* **1976**, 439–446.

[36] P. J. Stang, B. Olenyuk, A. M. Arif, *Organometallics* **1995**, *14*, 5281–5289.

[37] G. M. Sheldrick, Programs for the Refinement of Crystal Structures, University of Göttingen, Göttingen (Germany), **1996**.

[38] R. Hoffmann, *J. Chem. Phys.* **1963**, *39*, 1397–1412.

[39] J. H. Ammeter, H.-B. Bürgi, J. Thibeault, R. Hoffmann, *J. Am. Chem. Soc.* **1978**, *100*, 3686–3692.

Received: December 5, 2003
Published online: June 9, 2004

